January 2021

Assessing a Novel Adaptation to CCI Devices to Model Human Mild Traumatic Brain Injury

William R. Kochen
Nova Southeastern University, wkochen@nova.edu

Kristen Craven
George Mason University, kcrav97@gmail.com

Rachel E. Barkey
George Mason University, rbarkey@gmu.edu

Jane M. Flinn
George Mason University, jflinn@gmu.edu

David D. Cerri
George Mason University, dcerri@gmu.edu

Follow this and additional works at: https://nsuworks.nova.edu/neurosports

Part of the Exercise Science Commons, Neuroscience and Neurobiology Commons, and the Sports Sciences Commons

Assessing a Novel Adaptation to CCI Devices to Model Human Mild Traumatic Brain Injury

Abstract

Background: Traumatic Brain Injuries (TBIs) are a health crisis with over a million people suffering injuries each year in the United States. The majority of TBIs are mild injuries which often produce no period of unconsciousness and no gross damage to the brain or skull. A range of TBI animal models exist but many produce injuries too severe to characterize as mild. One TBI induction method commonly used is Controlled Cortical Impact (CCI) devices.

New Method: The purpose of this study is to assess a novel adaptation to CCI devices that allows for the induction of mild injuries that mimic human mild TBI (mTBI). In this apparatus, the mouse is placed on an elevated platform which utilizes a sensor to collapse the platform as the impactor hits the head.

Results: On the first day of injury, the repetitive dropping platform group had a significantly lower Time to Righting (TTR) than both control and single hit stationary platform groups. Additionally, on the first day of injury the single-hit stationary group had a significantly increased Time to Ambulation (TTA) compared to all other groups. Furthermore, this adaptation produces significantly less GFAP than CCI injuries performed without the falling platform.

Comparison with existing models: This model incorporates the high control of the CCI device that may be lost in weight-drop models of mild injury while also producing translational mild injuries.

Conclusion: This adaptation can be used in any CCI research lab to translationally study mild injuries. This will facilitate murine research into mTBI.

Keywords

Traumatic Brain Injury, Methods, Controlled Cortical Impact, Translation

Introduction

Traumatic Brain Injuries (TBIs) are responsible for over 250 thousand hospital visits or deaths annually in the United States (Langlois, et al., 2006; Center for Disease Control and Prevention, 2021). They are caused when an outside force exerts a form of direct physical damage to the brain. The source of this physical damage varies widely. Sources include blunt strikes to the head, explosions, penetrating injuries, road traffic accidents, and falls (Peeters et al., 2015; Center for Disease Control and Prevention, 2021). The severity of injury also has considerable variation, with milder injuries causing concussive symptoms and severe injuries causing coma and, in some cases, death. It is estimated that 75% of all TBIs fall under a classification of mild, with severe injuries being the minority (CDC-TBI Fact Sheet).

One challenging aspect of TBI experiments involving animal models is the translation of the model to human injuries (Levin & Robertson, 2012). TBIs, across varying degrees of severity in humans, happen to individuals while awake and often do not produce any period of unconsciousness. Furthermore, human mild TBIs often induce non-compressive forces on the brain (Cullen et al., 2016). Many animal models of TBI often induce a compressive injury on a deeply anesthetized mouse. Mice receiving these injuries remain unconscious and take significantly longer than control mice to right themselves following injury. The compressive forces inflicted using these models does not translate well to human mild injuries. Moreover, they are unable to model concussive TBI (also known as mild TBIS) which is often marked by no period of unconsciousness. However, mounting evidence indicates that multiple concussive injuries produce long-term behavioral difficulties as seen in athletes and military personnel.

Controlled Cortical Impact to induce mild injury

A major model used in TBI research is the Controlled Cortical Impact (CCI) device. A CCI device allows for a small impact to directly strike a location within the brain (Dixon, et al., 1991). These machines use electromagnetic coils and a computer delivery system to ensure that the same force is applied consistently for all injuries (Smith et al., 1995). Many of these machines have different diameter impact tips that can be used to simulate different types and severities of injuries. A craniotomy is often performed prior to CCI allowing for the machine to directly impact brain tissue.

The effect of craniotomy alone produces an equivalent amount of inflammatory protein release as the injury that follows (Lagraoui et al., 2012). Craniotomies allow researchers to know with great accuracy what area of the brain is being impacted; however, they are not translatable to the majority of TBI cases in humans. In human TBI, the skull is thought to absorb a fraction of the force of the injury and diffuse the injury throughout the brain, resulting in decreased damage to the focal point (Yoganandan et al., 1995; Kerr, 2013). Through removing the skull and

directly impacting the brain of the mouse, multiple parts of the normal human TBI experience are taken away. The results of these studies offer good insight into damage from penetrating injuries, as well as piercing blast damage, but are not considered to be good substitutes for mild TBI, which comprises over 75% of all TBI cases.

In recent years, labs with CCI devices have sought to use the machine on a closed skull to better replicate human TBI. When this is done with the mouse's head resting against a hard object, such as a stereotaxic base, the skull is compressed. This exacerbates injury pathology and makes it challenging to produce an injury like that of a concussion in humans. As human injuries typically involve acceleration, deceleration, and rotational forces during the initial injury rather than the compression injury that most of the current CCI devices induce (Daneshvar et al., 2015), the addition of the dropping platform allows for a better translation to human injuries. Adaptations, including placing the mouse on a soft platform and using a silicon impactor tip, have worked to reduce compression (Main et al., 2017). Nonetheless, injuries induced using closed-head CCI devices often impact mice under deep anesthesia and have difficulty producing concussive injuries.

The purpose of this study was to assess a novel apparatus, the Triggered Collapse Platform (TCP) – CCI (created by the last author), which reduces compressional forces and allows for the induction of mild injuries using a CCI. This device features a resettable fall-away platform which allows for ultra-mild injuries to be induced on mice undergoing light anesthesia.

The result is injuries which do not produce long periods of unconsciousness. The combination of low-anesthesia and non-compressive forces makes this model highly translational to concussive human injuries. As current research indicates long-term behavioral and neuronal pathologies following multiple mild injuries, the TCP-CCI should be useful in these studies.

To assess the validity of the device, this experiment conducted CCI impacts using the TCP-CCI modification with both the platform held still and the platform dropping away. Mice were monitored for time to establish the righting reflex. Additionally, levels of Glial Fibrillary Acidic Protein (GFAP) were assessed and cresyl violet staining and quantification was conducted. Time to righting (TTR) is the time it takes for the mouse to establish its four feet on the ground in a standing position post-injury. Increases in these times translate to longer periods of unconscious and disorientation following TBI in people which are indicative of more severe injuries. GFAP is an intermediate filament protein found in mature astrocytes which is released following astrocytic degeneration. GFAP levels have been found to highly correlate with injury severity (Pelinka et al., 2004) and serum GFAP levels are used to determine injury severity in human injuries.

Materials and Methods

All procedures were carried out in accordance with protocols approved by George Mason University's Institutional Animal Care and Use Committee and conducted in accordance with the NIH Guide to the Care and Use of Laboratory Animals. C57BL/6J mice were used in all the experiments in this study. All mice were given ad libitum access to food and water and on a 12:12 light dark cycle. To investigate the effect of the platform across multiple hits, 5 groups were used:

1) sham injury
2) single injury with stationary platform (smTBI stationary)
3) single injury with collapsing platform (smTBI collapsing)
4) five injuries with stationary platform (rmTBI stationary)
5) five injuries with collapsing platform (rmTBI collapsing).

Five mice were used in each group for behavior and histology except for single injury sham mice which were ten mice per group. All mice were 12 weeks old at the time of injury induction.

Description of the Device

This apparatus was designed to augment and extend the functionality of our existing Leica, Impact One impactor, so it could be used in studies of TBI over a wide range of severities, including mild and ultra-mild, with a predetermined and minimal amount of compressive force. The design allows for easy adjustment of numerous parameters, as well as easy set up/reset between trials.

Stereotaxic frame modifications

The *impactor solenoid* (Fig. 1, A) of a Leica, Impact One, Model #39463920, was mounted on the adjustable armature of a standard stereotaxic device. The impactor's velocity is adjustable between 1.5 m/s and 6 m/s. Other parts of the stereotax were repurposed, and custom parts were fabricated as needed. The stereotax's U-frame assembly was removed to make room for the new platform assembly. A custom *bracket* (Fig. 1, B) was attached to the original *baseplate* (Fig. 1**,** C) to allow repositioning of the stereotax's *micro-adjuster arm assembly* **(**Fig.1, D). The impactor mounting rod was attached to the end of the arm in a vertical orientation. The *lockable 2-axis joint (*Fig. 1, E), located at the base of the arm assembly, which was part of the original stereotax, enables the impactor to be positioned at varying angles away from vertical, allowing impact from different angles. The *three-arm assembly micro-adjusters* (Fig. 1, F) allow precise positioning of the *impactor plunger* (Fig. 1 & 3, G) over the target area.

Magnetic platform

A polycarbonate pan (Fig. 1, H) with *acrylic risers (*Fig. 1, J) was attached to the baseplate where the stereotax's U-frame assembly had been. The pan serves as support for *the collapsing platform* (Fig. 1 & 2, K) on which the mouse is placed, as well as providing a catchment area for the mouse after impact. Figure 2 shows the platform in the collapsed position. The platform is supported by *pivot screws* (Fig. 2, L). The pivot-screws loosely engage with holes in aluminum *support rails* (Fig. 2, M) which extend from the rear edge of the platform towards the front, on each side of the platform. In each rail are a series of holes, any opposing pair of which can be used to engage with the pivots. This permits rough adjustment of the platform's center of gravity. The platform collapses on the *axis of rotation* (Fig. 2, N), indicated by the line perpendicular to N. The radius of rotation the mouse undergoes upon impact is equal to the minimum distance (Figure 5 and 6) between the axis of rotation, and the point of impact. This distance is easily measured using a small ruler, and adjustment can accurately be made using the stereotax's *front/back micro-adjuster* (Fig. 2, O). On our device the radius of rotation is adjustable between 15mm and 50mm (for the current study, it was set at 18mm). Also attached to the baseplate is the *magnet micro-adjuster* (Fig. 2, P), repurposed from the original stereotax. The moving portion of the micro-adjuster carries a pair of rare-earth *magnets* (Fig. 2, Q), which, when the platform is in a level position, align with two *ferrous metal screws (*Fig. 2, R) on the back edge of the platform. The platform is kept level by the magnetic flux between the magnets and steel screws. By varying the distance between the magnets and screws with the micro-adjuster, the holding force can be accurately adjusted over a wide range. The greater the distance, the lower the holding force, and the smaller the impact force required to release the platform. The opposite is true for decreasing distances. A custom *two-part bracket* (Fig. 2,S), on which the micro-adjuster is mounted, allows adjustment of the level resting position of the platform by altering the height of the magnet micro-adjuster relative to the baseplate. The bracket can be locked in position when the platform is level. Using magnetic flux to maintain the platform position allows precise control over how much impact force is required before the mouse falls and eliminates any variability that might result from friction or stick-slip that might be introduced by methods involving physical contact.

A layer of foam can be placed in the catchment area to cushion the mouse's fall. Materials used for the catchment area and platform allow them to be easily cleaned and sanitized.

Platform solenoid and phototransistor trigger

To enable trials using low energies or very small impact depths, which might not have sufficient energy to release the platform, the apparatus employs an additional *platform solenoid* (Fig. 2,T), mounted under the rear edge of the platform. When energized, this solenoid (ZYE1-0530, 12VDC, 1A) forces the rear edge of the platform up, displacing its alignment with the magnets, weakening the flux, and causing the platform to fall. To trigger the platform solenoid, an emitter-detector pair (EDP) consisting of an *LED* (Fig. 3, V) and a *phototransistor* (Fig. 3, U) is utilized. The EDP is mounted on an *adjustable fixture* (Fig. 1 & 3, W) clamped to the side of the impactor solenoid. The EDP monitors motion of the impactor solenoid's plunger by sensing whether a *black band* (Fig. 3, X), painted around the plunger, has passed in front of the detector. The shiny stainless-steel plunger reflects light - the black band does not. The fixture allows positioning of

the EDP in 4 axes relative to the plunger and the black band, ensuring reliable triggering, and adjustment of desired latency between actuation of the impactor solenoid and triggering of the platform solenoid. Latency is adjusted by varying the distance, as measured along the length of the impactor plunger (i.e., along its direction of motion), between the EDP, and the black band. Once made, all adjustments can be locked.

Trigger circuit

The platform solenoid is triggered by a simple dark-detecting *electronic circuit* (schematic in Fig. 4), which is housed in a *plastic box* (Fig. 2, Y) attached to the polycarbonate pan. A phototransistor (NPN Infrared 276-0145) is mounted on an adjustable holder side-by-side with a white-light emitting 5mm LED (3V, 20mA, HM-13052), which provides steady illumination of the plunger. Light emitted through the side of the LED package is shielded from entering directly through the side of the phototransistor package, so the phototransistor primarily 'detects' only light reflected off the plunger. Current to the LED is limited by a 450 Ohm resistor. The EDP is connected to the rest of the circuit by a *cable* (Fig. 1 & 2, Z). When the impactor solenoid is energized, the dark band painted around the plunger moves in front of the EDP, reducing the light signal reflected onto the phototransistor's base. The phototransistor's collector is connected to the gate of a MOSFET (N-channel 276-2072/IRF510), and to a 100K resistor. The other side of the resistor is connected via a single-pole/single-throw *on/off switch* (Fig. 2, AA) to +12VDC. One side of the platform solenoid is connected to the MOSFET's drain, and the other side via the on/off switch to +12VDC. The MOSFET's source, and the phototransistor's emitter are at ground. The circuit is powered by a standard A/C adapter which has 12VDC output.
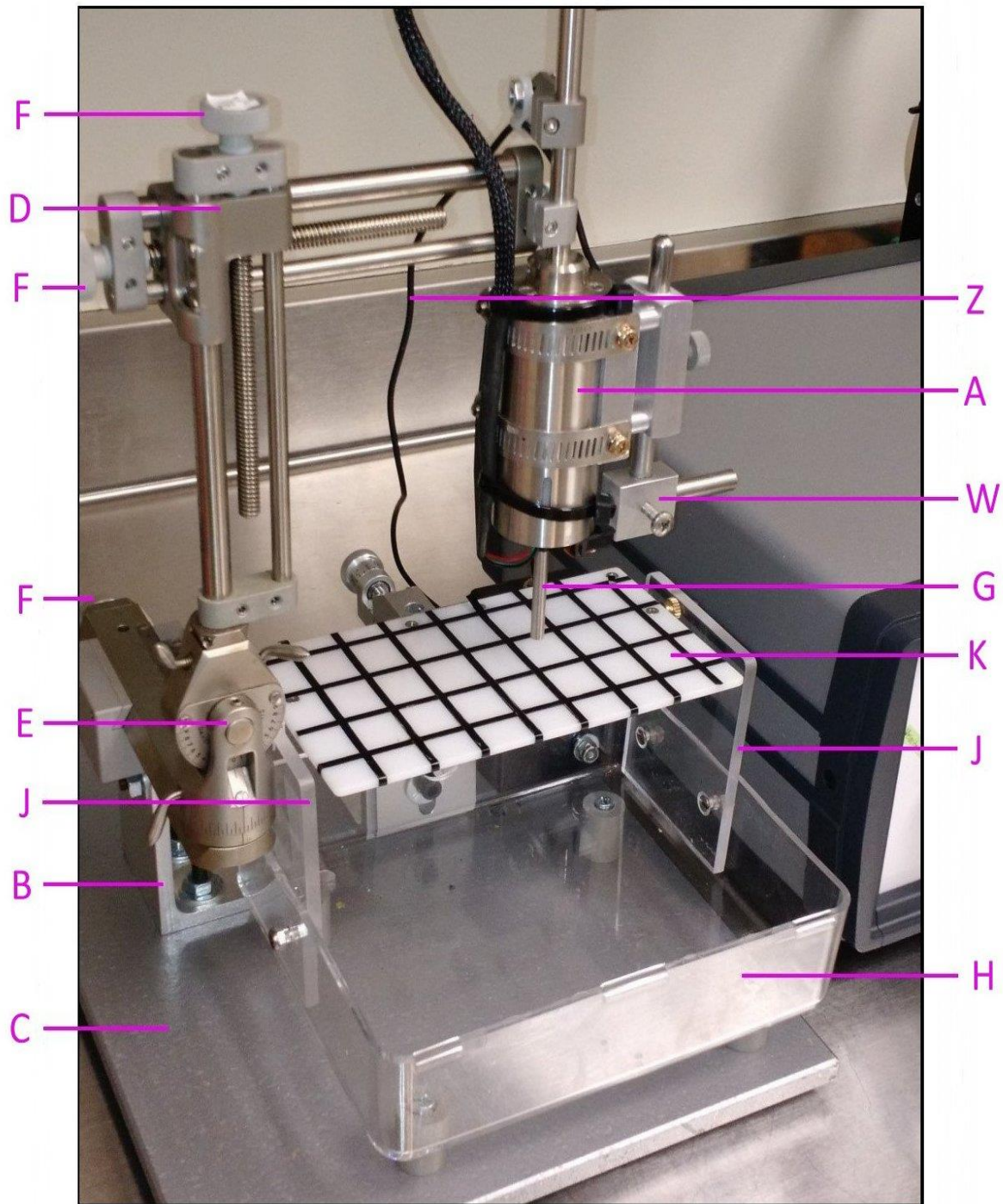
Figure 1. Triggered collapse platform, front view. A = Impactor solenoid; B = Bracket; C = Baseplate; D = Micro-adjuster arm assembly; AB = Impactor mounting rod; E = Lockable 2-axis joint; F = Arm assembly micro-adjusters; G = Impactor plunger; H = Polycarbonate pan; J = Acrylic risers; K = Collapsing platform; W = Adjustable fixture; Z = Cable
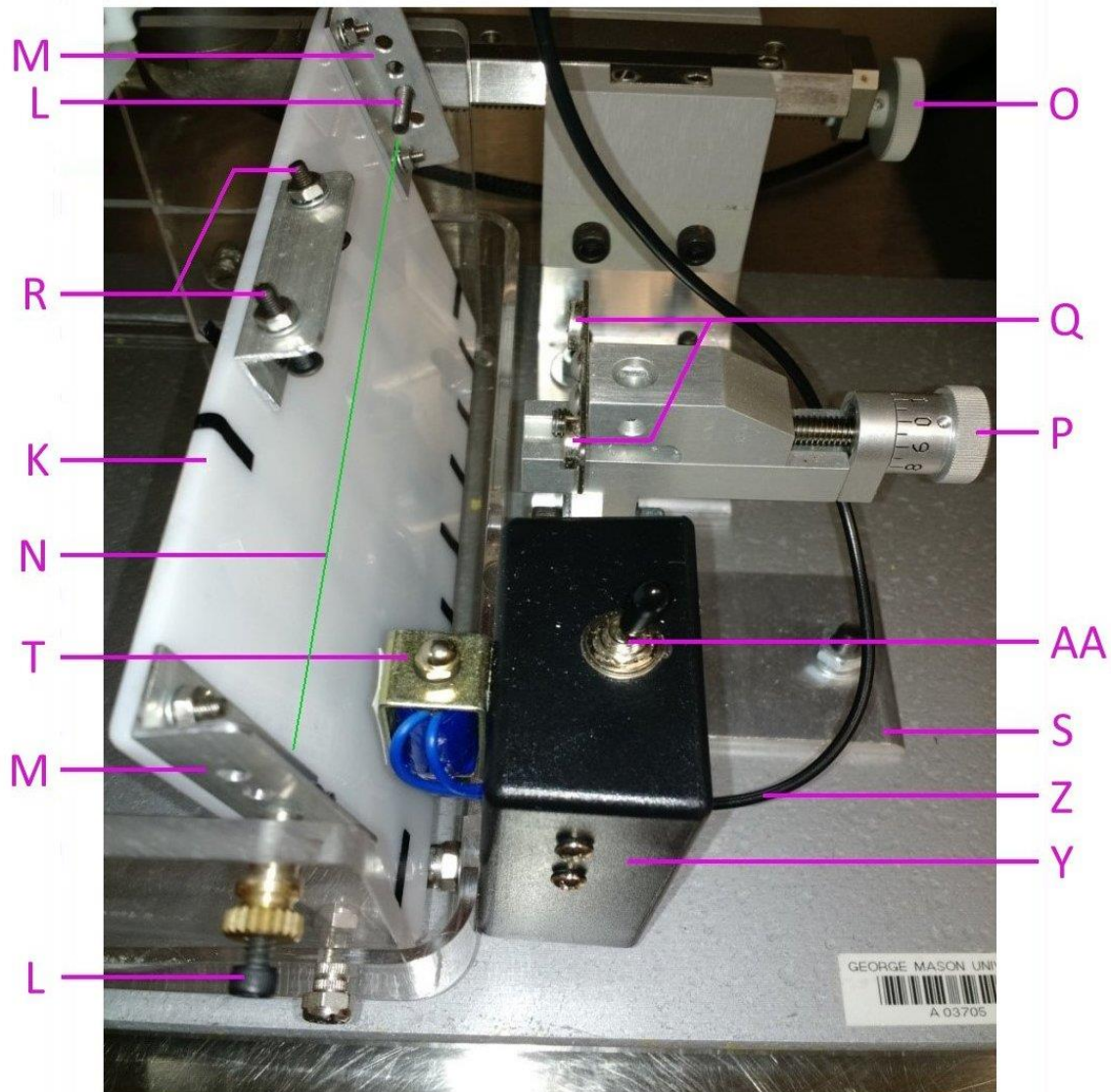
Figure 2. Top view of platform mechanism (in collapsed position) K = Collapsing platform; L = Pivot screws; M = Support rails; N = Axis of rotation; O = Front/back micro-adjuster; P = Magnet micro-adjuster; Q = Magnets; R = Ferrous metal screws; S = Two-part bracket; T = Platform solenoid; Y = Plastic box; Z = Cable; AA = On/off switch
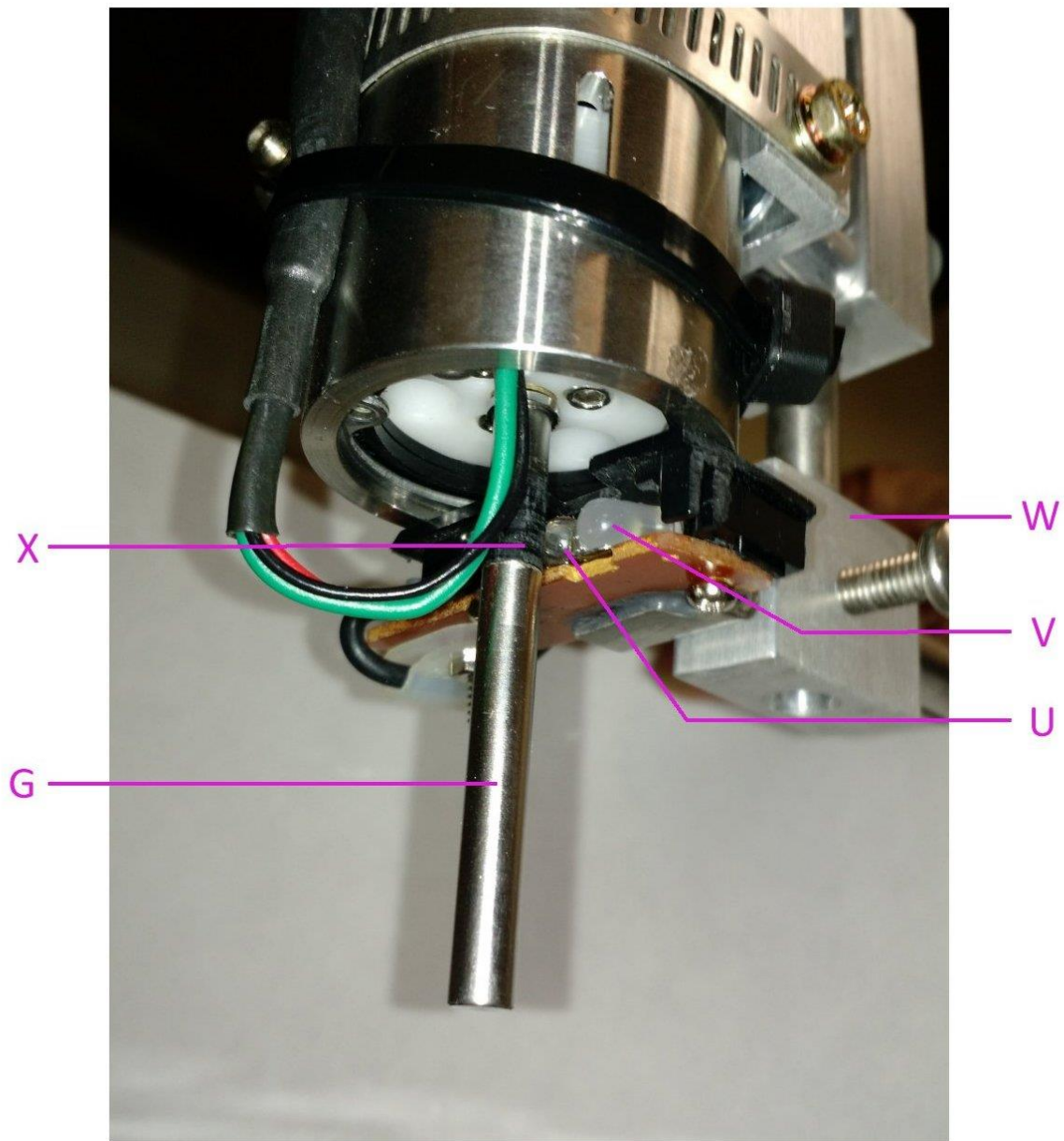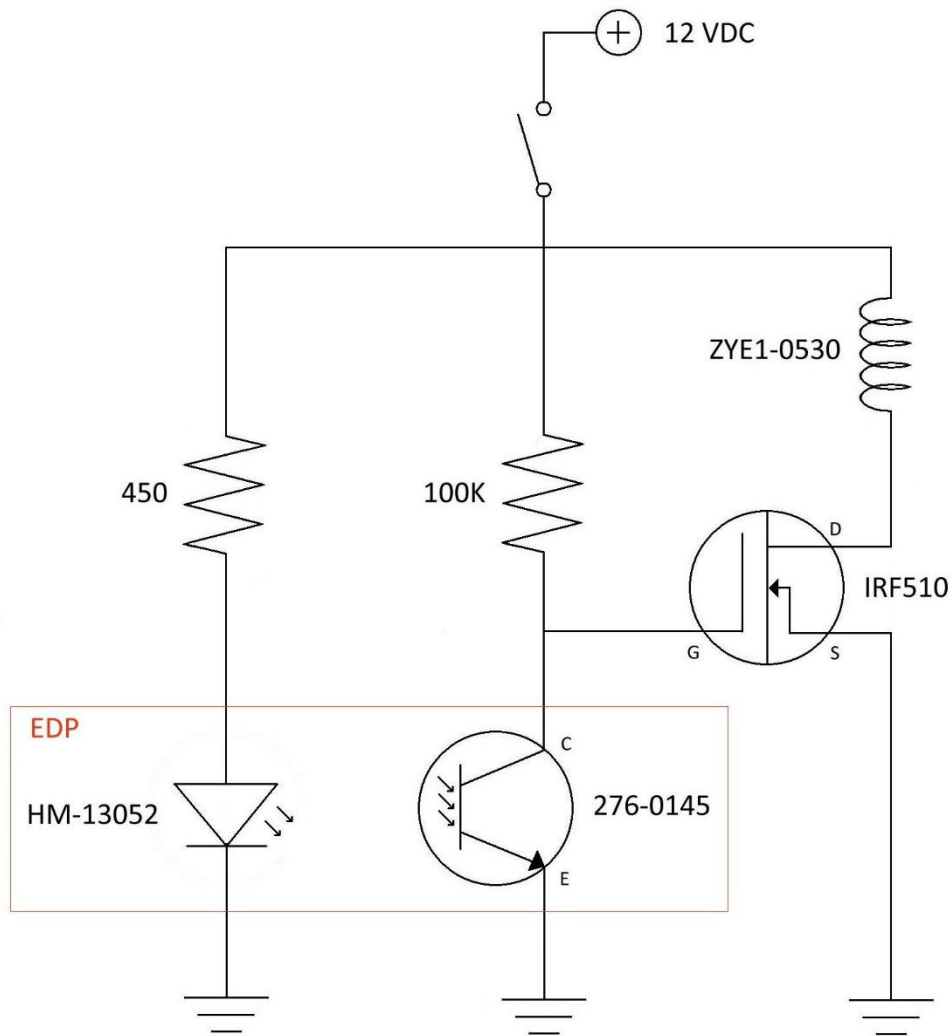
Figure 3. Close-up of impactor showing triggering components. G = Impactor plunger; T = Platform solenoid; V = LED; U = Phototransistor; W = Adjustable fixture; X = Black band

Platform Solenoid Circuit

Figure 4.

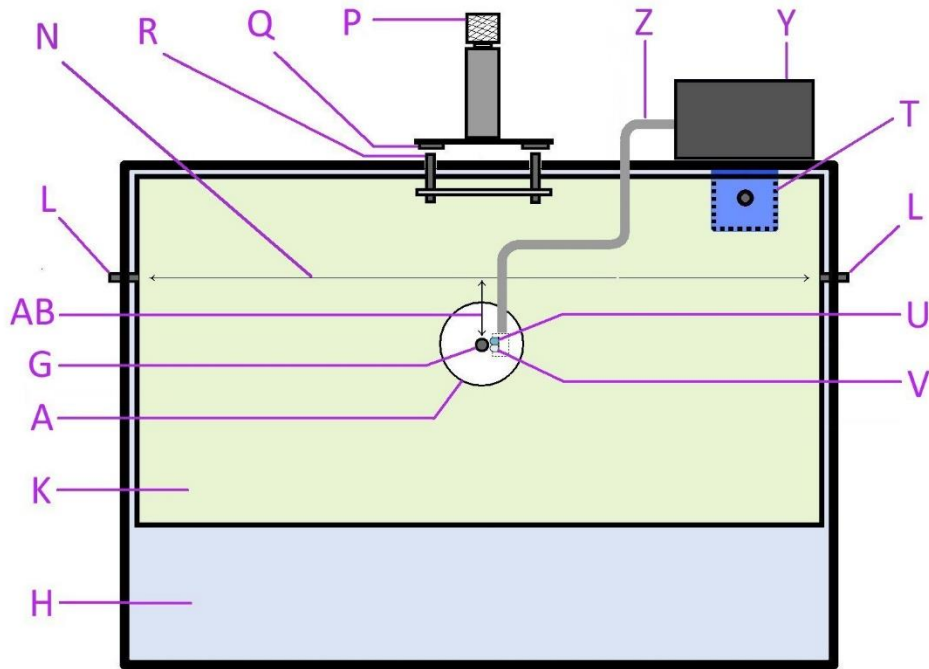**Figure 5.** Diagram top view. A = Impactor solenoid; G = Impactor plunger; H = Polycarbonate pan; K = Collapsing platform; L = Pivot screws; N = Axis of rotation; Q = Magnets; P = Magnet micro-adjuster; R = Ferrous metal screws; T = Platform solenoid; U = Phototransistor; V = LED; Y = Plastic box; Z = Cable; AB = Minimum distance. (NOTE: Not to scale. Not all parts labeled in photos are labeled in diagram.)

Figure 6. Side view diagram. A = Impactor solenoid; G = Impactor plunger; H = Polycarbonate pan; J = Acrylic riser; K = Collapsing platform; L = Pivot screws; P = Magnet micro-adjuster; Q = Magnet; R = Ferrous metal screw; T = Platform solenoid; U = Phototransistor; V = LED; Y = Plastic box; Z = Cable; AB = Minimum distance. (NOTE: Not to scale. Not all parts labeled in photos are labeled in diagram.)

TBI Induction

C57BL/6J mice (The Jackson Laboratory) were anesthetized until unconscious to paw/tail pinch with 5% isoflurane. After becoming unresponsive, mice were transferred to nose cone anesthesia at 1.5% and positioned on top of platform. The CCI device was positioned so that the induction tip was directly over lambda, and nose cone anesthesia was removed. Thirty seconds after removal of anesthesia, the device was triggered causing TBI induction at 3m/s and a depth of 5mm. For the dropping group, when the hit was induced, the mice fell into the polycarbonate pan. For the stationary group, the platform was tightened so that it did not fall.

Time to Right and Ambulate

After each injury, blind observers using a stopwatch recorded how long it took the mice to right themselves. Timing was started as soon as the TBI or sham induction occurred. Sham mice and those with a stationary platform were gently moved from the platform into the polycarbonate pan. The sham mice were moved when the signal was given that would have started the CCT device. The Righting was defined as standing on all four feet. Ambulation was considered as taking the first step after righting. Mice were euthanized 24 hours after the final injury and brains were extracted.

Western Blot analysis of GFAP

Brain tissue was extracted and immediately frozen on dry ice (n = 4 per group). Samples were stored in a –80◦C freezer until homogenized. The left hemisphere was placed in 1mL of RIPA buffer on ice with Halt Protease and Phosphatase Inhibitor Cocktail (Thermo Fisher Scientific) at the recommended concentration of 10 µL/mL. Samples were homogenized and subsequently centrifuged at 14,000 RPM for 20 min at 4◦C and aliquoted. The BCA assay was run to determine protein concentrations. Samples were prepared using 40µg of protein, 2.5µL NuPAGE sample reducing agent, 6.25 µL LDS sample buffer, and 1x PBS for a final concentration of 25 µL. Samples were placed in a 37◦ C water bath for 30 min and loaded into NuPAGE 4–12% Bis-Tris gels in MOPS running buffer. SeeBlue Plus2 protein ladder was used to visualize molecular weight (Thermo Fisher Scientific). The gel was run at 120V for approximately 2 h and then transferred using the iBlot 2 Transfer System with mini nitrocellulose transfer stacks (Novex). The membrane was washed with PBST for 3 min and then blocked in 5% milk for 45 min with agitation.

Membranes were incubated with the primary antibodies at 4◦C in 2.5% milk block. GFAP was used a primary antibody (Thermo Fisher Scientific: Catalog # MA5-12023) and GapDH was used as a loading control (Thermo Fisher Scientific: Cat #MA5-15738). After primary antibody incubation, membranes were washed with PBST 3 times for 10 min each, and then placed in 2.5% milk block for 30 min. Membranes were incubated with HRP conjugated secondary antibody (1:20,000 Goat anti-rabbit Super clonal; Thermo Fisher Scientific) and then washed with PBST 3 times for 10 min each. Westpico PLUS chemiluminescent substrate (SuperSignal) was used for 4 min and blots were subsequently imaged with an exposure time of 8s. Images were semi-quantified using ImageJ (NIH) by calculating adjusted relative densities of bands.

One animal brain per group was not used in Western Blot due to an error in homogenization of tissue which was rectified.

Cresyl-Violet

24 hours after the final injury brains were extracted and flash frozen over dry ice (n=5 per group). Fresh frozen brain tissue was sliced at 16μm using a Leica CM3050S cryostat and mounted onto charged microscope slides (SuperFrost Plus Slides, Fisher Scientific). Slices were taken from the infralimbic region of the frontal cortex at ~ bregma 1.39mm anterior to the injury site and from hippocampal regions at ~2.54mm past bregma. From hippocampal slices, six brain regions were analyzed: dentate gyrus (DG), CA1 and CA3 regions, midline corpus callosum, the entorhinal and perirhinal cortex and the parietal association cortex. White matter density was also analyzed at midline corpus callosum. Slices were then stained with LuxolFastBlue/Cresyl-Violet solution.

Data Analysis

All data was analyzed using SPSS. Cresyl Violet was analyzed using one-way ANOVAs. GFAP was analyzed using a 2(number of hits) x 2 (platform condition) ANOVA. The sham group was not analyzed for GFAP. Time to righting and time to ambulation over four days was analyzed using a 3(condition) x 4(injury number) mixed measures ANOVA. Day one TTR and TTA were calculated using an ANOVA. All data were analyzed using $p<0.05$ as the cutoff for significance, and $p < 0.10$ to indicate a trend. Error bars represent standard error of mean in all graphs

Results

Time to Righting

On the first day of TBI Induction there was a significant difference found between groups (F (4,25) = 2.972, p = .039) (Figure 7a). Post-hoc analysis via Fisher's least significant difference found that the repeated dropping group had a significantly reduced TTR compared to sham (p = .003) and single stationary (p = .018), and a trending reduced TTR compared to repeated stationary (p = .055) and repeated dropping (p = .078). Over days 2-5 of TBI induction there was a significant between group difference found (F (2,12) = 5.230, p = .023) with pairwise comparisons showing the repetitive dropping group having a significantly reduced TTR compared to sham (p = .007) and a trending reduction compared to repetitive stationary (p =
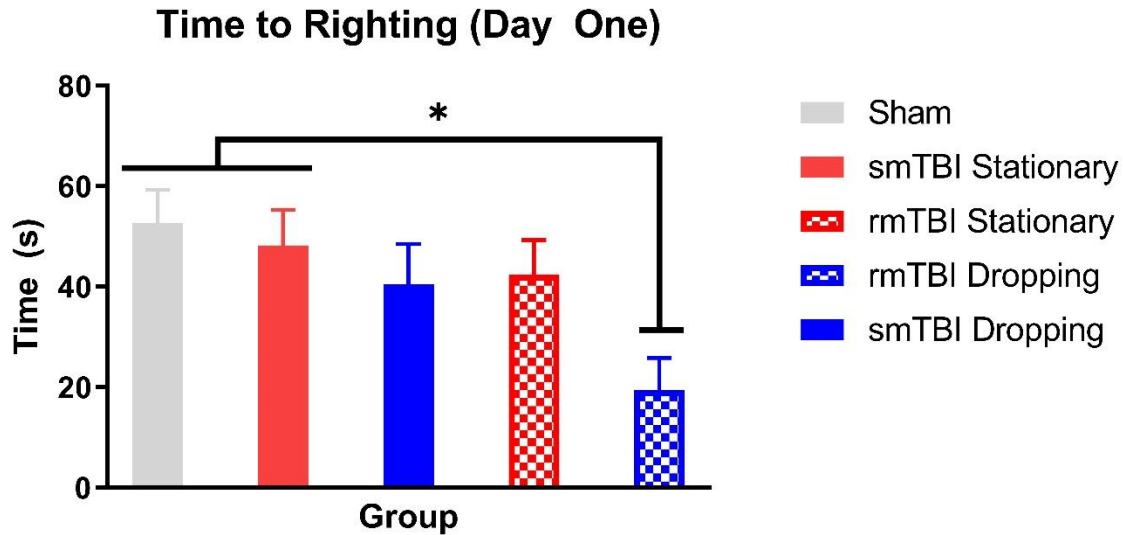
.078) (Figure 7b).

Time to Righting (Day One)

Figure7a. TBI Day One. On the first day of TBI Induction there was a significant difference found between groups (F (4,25) = 2.972, p = .039). Post-hoc analysis via LSD found that the repeated dropping group had a significantly reduced TTR compared to sham (p = .003) and single stationary (p = .018), and a trending reduced TTR compared to repeated stationary (p = .055) and repeated dropping (p = .078).
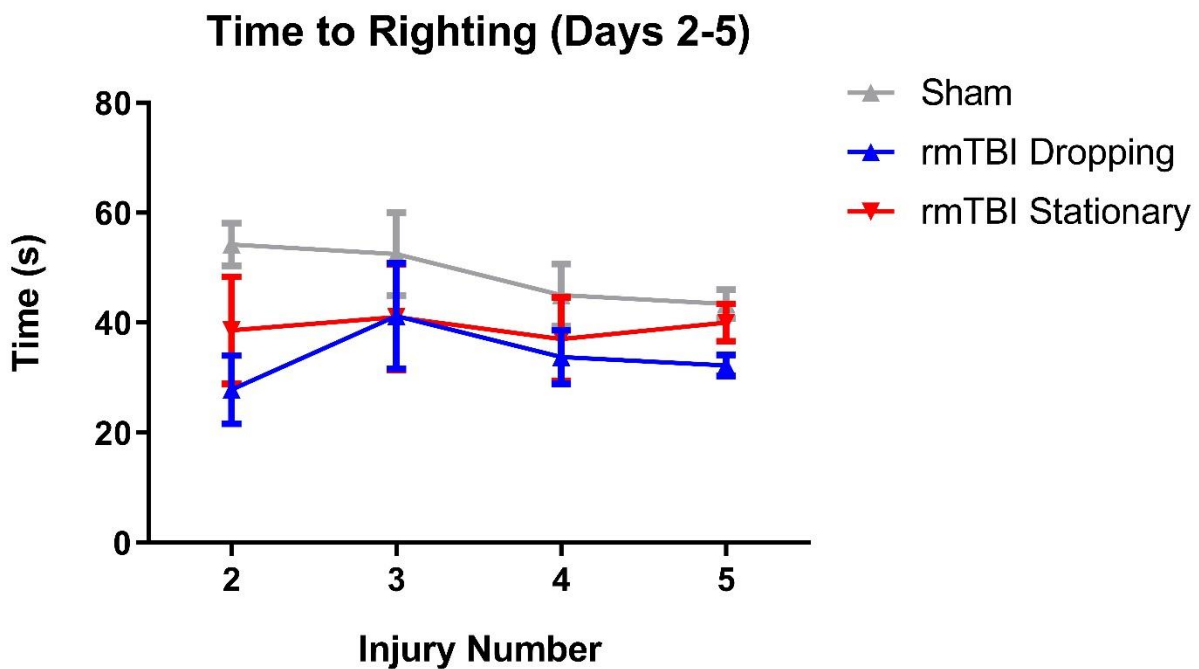
Time to Righting (Days 2-5)

Figure 7b. Over days 2-5 of TBI induction there was a significant between group difference found (F (2,12) = 5.230, p = .023) with pairwise comparisons showing the repetitive dropping

group having a significantly reduced TTR compared to sham ($p = .007$) and a trending reduction compared to repetitive stationary ($p = .078$)

Time to Ambulation

On the first day of TBI induction, there was a significant difference found between groups in time to ambulation ($F_{(4,25)} = 3.410$, $p = .023$) with LSD post-hoc analysis showing the single stationary group had a significantly increased TTR compared to all other groups: sham ($p = .015$), single dropping *($p = .006$), repeated stationary ($p = .011$), repeated dropping ($p = .004$)* (Figure 8a). There was no significant difference found in ambulation over days 2-5 ($F_{(2,12)}$, $p = .724$) (Figure 8b).
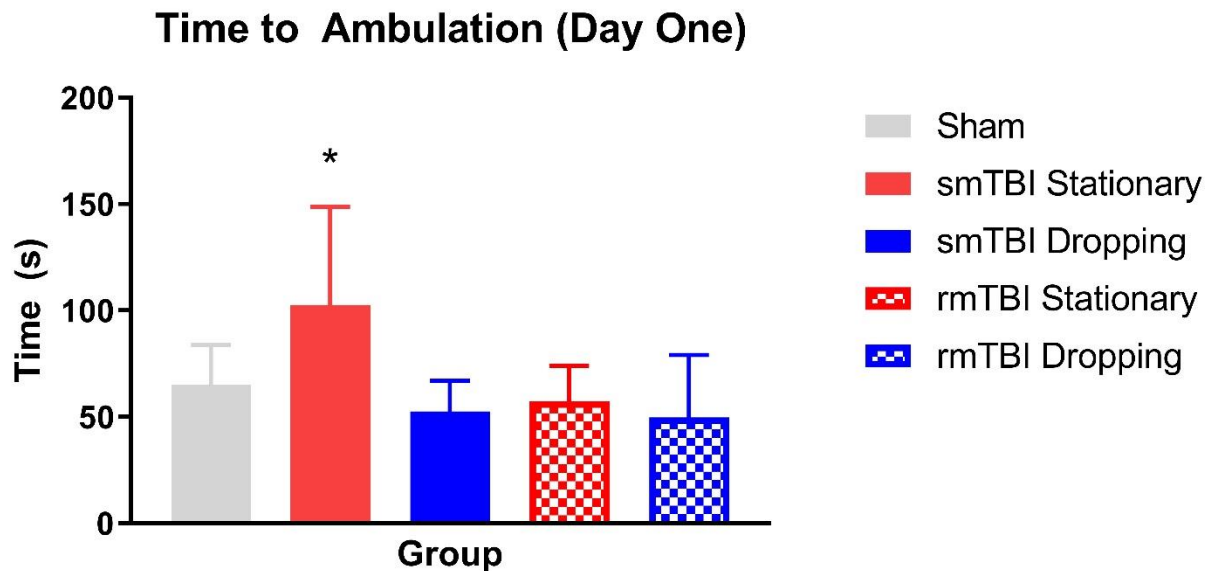

Figure 8a. On the first day of TBI induction, there was a significant difference found between groups in time to ambulation ($F_{(4,25)} = 3.410$, $p = .023$) with LSD post-hoc analysis showing the single stationary group had a significantly increased TTR compared to all other groups: sham ($p = .015$),single dropping *($p = .006$), repeated stationary ($p = .011$), repeated dropping ($p = .004$)*
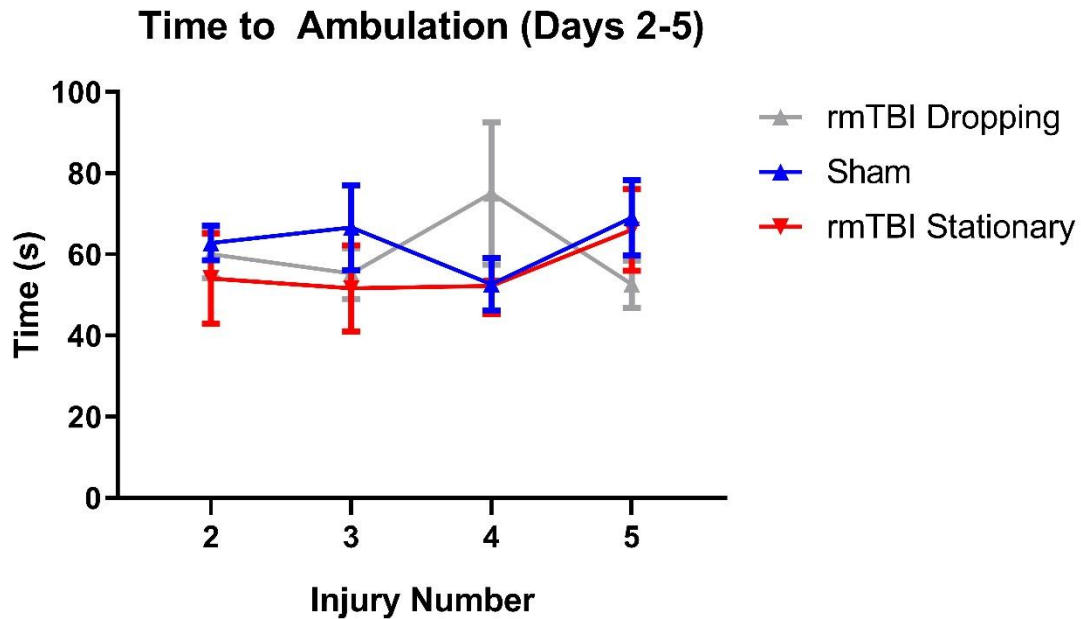
Figure 8b. There was no significant difference found in ambulation over days 2-5 (F (2,12), $p =$ .724)

Glial Fibrillary Acidic Protein

Levels of GFAP were accessed via Western blot with values normalized to GapDH. There was a significant increase in levels of GFAP caused by the number of hits F (1, 12) = 19.740, $p =$ .001, as well as a significant increase when the platform did not fall F (1, 12) = 11.876, $p =$ .005.

GFAP

Legend:
- smTBI Dropping
- rmTBI Stationary
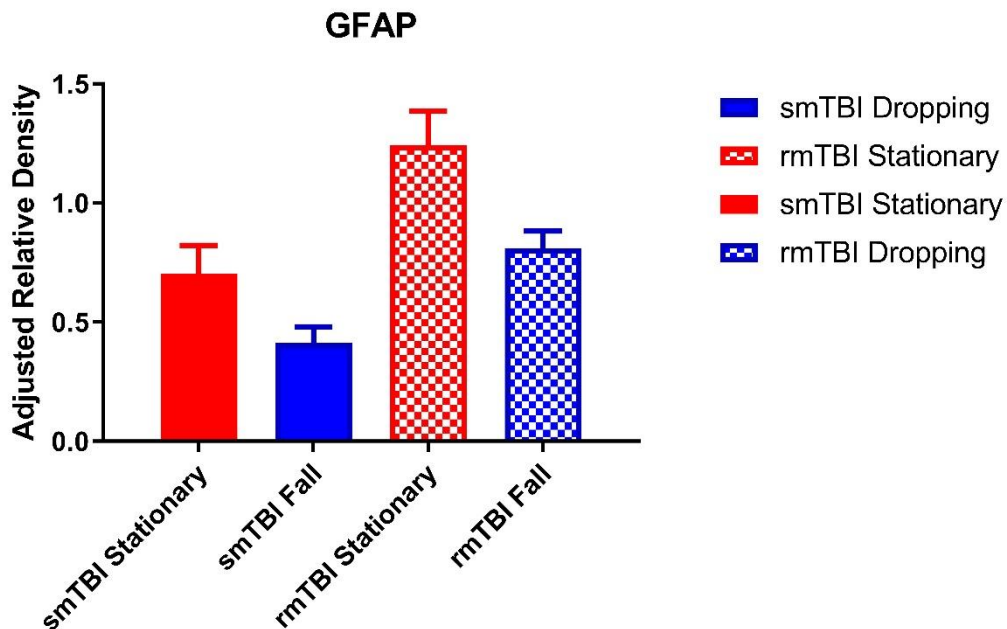- smTBI Stationary
- rmTBI Dropping

Figure 9. *GFAP levels were significantly increased by the number of injuries $F (1, 12) = 19.740$, $p = .001$, as well as increased when the platform did not fall $F (1, 12) = 11.876$, $p = .005$.*

Cresyl-Violet

No significant differences were found in any of the brain regions assessed ($p > 0.05$). Cell loss was trending significantly in the DG ($F (1, 24) = 2.76$, $p = 0.056$), with mice who sustained repetitive dropping TBI showing the lowest cell density.
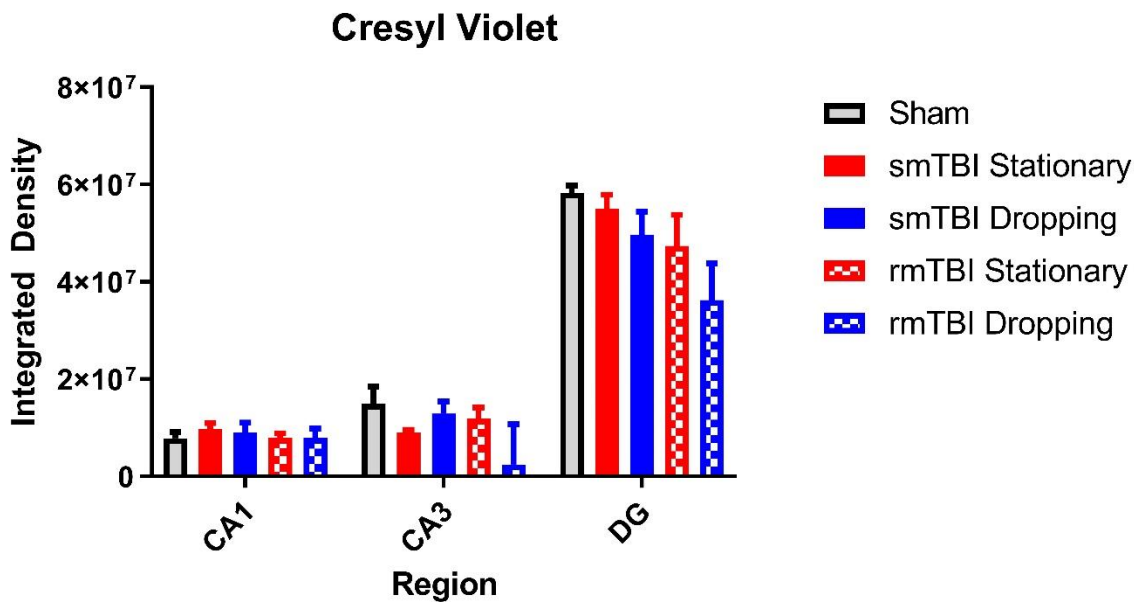

Cresyl Violet

Legend:
- Sham
- smTBI Stationary
- smTBI Dropping
- rmTBI Stationary
- rmTBI Dropping

Figure 10: Integrated Cell Density of Hippocampal Regions**.** There were no significant differences in cell density across TBI administrations in hippocampal regions. In the DG, cell density values were trending significantly with rmTBI with a dropping platform showing the lowest cell density compared to sham (p = 0.056)
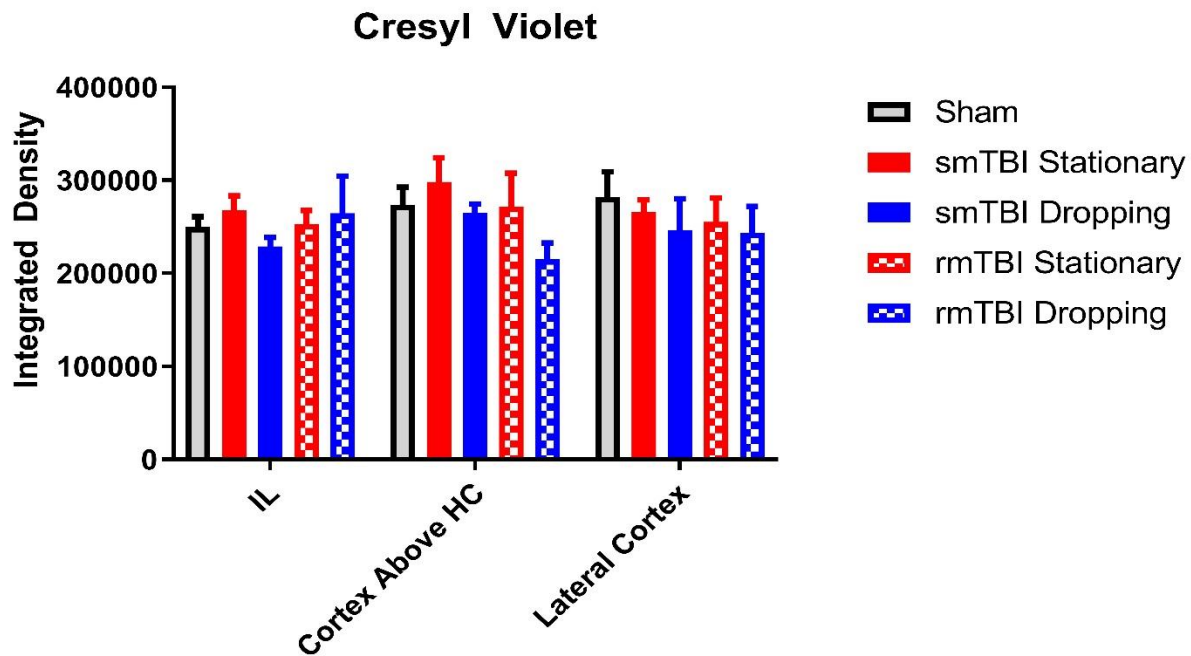

Figure 11. Integrated Cell Density of Cortical Regions. There were no significant differences in cell density across TBI administrations in cortical regions.

Discussion

The purpose of this study was to examine the effect of an adaptation to the widely used CCI device that allows for the induction of mild injuries which mimic clinically relevant symptoms. The TCP-CCI adaptation worked 100% of the time with the platform always falling away when the injury was induced. Furthermore, there was no mortality; no skull fracture and no cranial edema after injuries were induced in any groups. Other methods of inducing TBI often produce either direct mortality or indirect mortality via skull fracture forcing euthanasia (Marmarou et al., 1994). The reliability and mild induction of injury reinforce the translation of this device for mild injuries.

Mild human injuries often present with minimal-to-no post-injury unconsciousness. This is often missing from animal models which impose long periods of pre-injury anesthesia followed by long post-injury unconsciousness. Length and type of anesthesia have been found to significantly alter TBI pathology (Statler et al., 2006). TTR is often used in TBI studies to determine how severe an injury is based on how long it takes the animal to recover from injury and take its first step. In other methods of mTBI, righting time is extended, with mice taking several minutes to regain the righting reflex (Creeley et al., 2004; Kane et al., 2012; Mouzon et al., 2012). With this method, mice sustain a milder injury than other methods, with all injury groups taking less than a minute to regain the righting reflex. In this experiment, when the platform fell, the average time to right was lowest in the group that had the dropping platform. It was surprising that the sham group had the longest TTR; this injury being more mild than other TBI methodologies may explain the shorter TTR for injured groups.

A range of devices are currently used to induce TBIs in animals. The original weight drop model developed by Marmarou (1994) utilizes a weight that drops through a tube to strike an animal. Some experimenters utilize a helmet in these experiments while others do not. This method usually has the bottom of the head placed against a hard surface which increases compressive forces on the brain, reducing translational efficacy. The Kane adaptation to the weight-drop device which uses a foil cradle for the animal reduces compression but has been shown to increase righting time significantly.

The Closed-Head Impact Model of Engineered Rotational Acceleration (CHIMERA) uses rapid acceleration to induce a TBI. CHIMERA utilizes minimal anesthesia and preliminary evidence indicates it produces translational mTBI (Namjoshi et al., 2014). CHIMERA devices produce translational mTBIs but must be constructed or purchased and cannot be made using existing laboratory equipment such as the ubiquitous CCI device. Unmodified CCI and FPI devices induce strong focal injuries under deep anesthesia and often involve the use of a craniotomy. The current TCP-CCI modification will allow for researchers who already own a CCI device to cost-effectively transition to translational mild injuries.

The TCP-CCI adaptation resulted in the production of significantly less GFAP than the device with the platform stationary. There was also a significant effect of number of injuries causing an increase in GFAP, which is to be expected as subsequent injuries have been found to increase GFAP (Pelinka et al., 2004). Reduced GFAP levels following injury indicate that the TCP-CCI produced less severe injuries than traditional CCI injuries which, even without a craniotomy, produced higher levels of GFAP.

One interesting finding in this study was the significant decrease in time to righting found in the groups that received a TBI compared to sham control. This finding is not consistent with the majority of the literature which shows either an equal or significantly increased Time To

Righting for the injured groups. The majority of TBI research induces injuries on rats who are actively under general anesthesia which can have neuroprotective or exacerbating effects (Hoogenboom, Branch, and Lipton, 2019; Wojnarowicz et al., 2017). We hypothesize that the reduced time to righting in the injured groups is due to the interaction between post-anesthesia TBI and mild concussive mechanisms. One potential mechanism isoflurane anesthesia uses to exert its effects is through reducing cytokine production and reactive oxygen species (Neag et al., 2020). Following the removal of anesthesia, the effects of isoflurane slowly wear off and the brain returns to its resting state. The induction of a mTBI 30 seconds after the anesthesia has been removed may induce acute inflammation and neuronal excitability that causes the anesthetic effects to wear off faster.

The reduction in time to righting as well as reduced GFAP indicates that this adaptation allows for CCI devices to induce injuries that translationally duplicate the injuries found in many human clinical cases of mild TBI. CCI devices are used in many research labs throughout the world, with numerous attempts made to reduce injury severity while retaining reliability and reproducibility. Given that the majority of all human injuries are mild injuries that produce little-to-no unconsciousness, this adaptation will further both basic and therapeutic interventions by researchers.

Author Disclosure Statement
No competing financial or personal interests exist for any of the authors in this study. A patent application has been filed for this device.

References:

Centers for Disease Control and Prevention (2021). Surveillance Report of Traumatic Brain Injury-related Hospitalizations and Deaths by Age Group, Sex, and Mechanism of Injury—United States, 2016 and 2017. Centers for Disease Control and Prevention, U.S. Department of Health and Human Services.

Creeley, C. E., Wozniak, D. F., Bayly, P. V., Olney, J. W., & Lewis, L. M. (2004). Multiple Episodes of Mild Traumatic Brain Injury Result in Impaired Cognitive Performance in Mice. *Academic Emergency Medicine*, 11(8), 809–819. https://doi.org/10.1197/j.aem.2004.03.006

Cullen, D.K., Harris, J.P., Browne, K.D., Wolf, J.A., Duda, J.E., Meaney, D.F., Margulies, S.S. and Smith, D.H., 2016. A porcine model of traumatic brain injury via head rotational acceleration. *In Injury Models of the Central Nervous System* (pp. 289-324). Humana Press, New York, NY. https://doi.org/10.1007/978-1-4939-3816-2_17

Daneshvar, D. H., Goldstein, L. E., Kiernan, P. T., Stein, T. D., & McKee, A. C. (2015). Post-traumatic neurodegeneration and chronic traumatic encephalopathy. *Molecular and Cellular Neuroscience*, 66, 81–90. https://doi.org/10.1016/j.mcn.2015.03.007

Dixon, E. C., Clifton, G. L., Lighthall, J. W., Yaghmai, A. A., & Hayes, R. L. (1991). A Controlled cortical impact model of traumatic brain injury in the rat. Journal of Neuroscience Methods, 39(3), 253–262. https://doi.org/10.1016/0165-0270(91)90104-8

Hoogenboom, W.S., Branch, C.A. and Lipton, M.L., 2019. Animal models of closed-skull, repetitive mild traumatic brain injury. *Pharmacology & therapeutics*, 198, pp.109-122. https://doi.org/10.1016/j.pharmthera.2019.02.016

Kane, M. J., Angoa-Pérez, M., Briggs, D. I., Viano, D. C., Kreipke, C. W., & Kuhn, D. M. (2012). A mouse model of human repetitive mild traumatic brain injury. Journal of Neuroscience Methods, 203(1), 41–49. https://doi.org/10.1016/j.jneumeth.2011.09.003

Kerr, H. A. (2013). Closed Head Injury. *Clinics in Sports Medicine*, 32(2), 273–287. https://doi.org/10.1016/j.csm.2012.12.008

Lagraoui, M., Latoche, J. R., Cartwright, N. G., Sukumar, G., Dalgard, C. L., & Schaefer, B. C. (2012). Controlled Cortical Impact and Craniotomy Induce Strikingly Similar Profiles of Inflammatory Gene Expression, but with Distinct Kinetics. *Frontiers in Neurology*, 3. https://doi.org/10.3389/fneur.2012.00155

Langlois, J. A., Rutland-Brown, W., & Wald, M. M. (2006). The epidemiology and impact of traumatic brain injury: a brief overview. *The Journal of Head Trauma Rehabilitation*, 21(5), 375-378.

Levin, H. S., & Robertson, C. S. (2012). Mild Traumatic Brain Injury in Translation. *Journal of Neurotrauma*, 30(8), 610–617. https://doi.org/10.1089/neu.2012.2394

Marmarou, A., Foda, M. A. A.-E., Brink, W. Van Den, Campbell, J., Kita, H., & Demetriadou, K. (1994). A new model of diffuse brain injury in rats. *Journal of Neurosurgery*, 80(2), 291–300. https://doi.org/10.3171/jns.1994.80.2.0291

Main, B. S., Sloley, S. S., Villapol, S., Zapple, D. N., & Burns, M. P. (2017). A Mouse Model of Single and Repetitive Mild Traumatic Brain Injury. *Journal of Visualized Experiments: JOVE,* (124). https://doi.org/10.3791/55713

Mouzon, B., Chaytow, H., Crynen, G., Bachmeier, C., Stewart, J., Mullan, M., Stewart, W., & Crawford, F. (2012). Repetitive mild traumatic brain injury in a mouse model produces learning and memory deficits accompanied by histological changes. *Journal of Neurotrauma*, 29(18), 2761–2773. https://doi.org/10.1089/neu.2012.2498

Namjoshi, D.R., Cheng, W.H., McInnes, K.A., Martens, K.M., Carr, M., Wilkinson, A., Fan, J., Robert, J., Hayat, A., Cripton, P.A. and Wellington, C.L., 2014. Merging pathology with biomechanics using CHIMERA (Closed-Head Impact Model of Engineered Rotational Acceleration): a novel, surgery-free model of traumatic brain injury. *Molecular neurodegeneration*, 9(1), pp.1-18. https://doi.org/10.1186/1750-1326-9-55

Neag, M. A., Mitre, A. O., Catinean, A., & Mitre, C. I. (2020). An Overview on the Mechanisms of Neuroprotection and Neurotoxicity of Isoflurane and Sevoflurane in Experimental Studies. *Brain Research Bulletin*. https://doi.org/10.1016/j.brainresbull.2020.10.011

Pelinka, L. E., Kroepfl, A., Leixnering, M., Buchinger, W., Raabe, A., & Redl, H. (2004). GFAP versus S100B in serum after traumatic brain injury: relationship to brain damage and outcome. *Journal of Neurotrauma*, 21(11), 1553–1561. https://doi.org/10.1089/neu.2004.21.1553

Peeters, W., van den Brande, R., Polinder, S., Brazinova, A., Steyerberg, E.W., Lingsma, H.F. and Maas, A.I., (2015). Epidemiology of traumatic brain injury in Europe. *Acta neurochirurgica*, 157(10), pp.1683-1696. https://doi.org/10.1007/s00701-015-2512-7

Smith, D. H., Soares, H. D., Pierce, J. S., Perlman, K. G., Saatman, K. E., Meaney, D. F., … McIntosh, T. K. (1995). A model of parasagittal controlled cortical impact in the mouse: cognitive and histopathologic effects. *Journal of Neurotrauma*, 12(2), 169–178. https://doi.org/10.1089/neu.1995.12.169

Statler, K. D., Alexander, H., Vagni, V., Dixon, C. E., Clark, R. S., Jenkins, L., & Kochanek, P. M. (2006). Comparison of seven anesthetic agents on outcome after experimental traumatic brain injury in adult, male rats. *Journal of Neurotrauma*, 23(1), 97-108. https://doi.org/10.1089/neu.2006.23.97

Wojnarowicz, M. W., Fisher, A. M., Minaeva, O., & Goldstein, L. E. (2017). Considerations for experimental animal models of concussion, traumatic brain injury, and chronic traumatic encephalopathy—these matters matter. *Frontiers in neurology*, 8, 240. https://doi.org/10.3389/fneur.2017.00240

Yoganandan, N., Pintar, F.A., SANCES JR, A.N.T.H.O.N.Y., Walsh, P.R., Ewing, C.L., Thomas, D.J. and Snyder, R.G., 1995. Biomechanics of skull fracture. Journal of neurotrauma, 12(4), pp.659-668. https://doi.org/10.1089/neu.1995.12.659.